

# Microstructure and thermal conductivity of AlN ceramics containing additives

SHUAI DU, LONGQIAO GAO, FA LI, ZHENG LIU

*Beijing Vacuum Electronics Research Institute, P.O. Box 749, Beijing 100016, P.R. China*

YOUNG JEI-OH

*Korea Institute of Science and Technology, P.O. Box 131, Cheongryang, Seoul 130-650, Korea*

The effect on AlN ceramic of the addition of  $Y_2O_3$ ,  $Yb_2O_3$ ,  $Er_2O_3$  and CaO were investigated using scanning electron microscopy (SEM), transmission electron microscopy (TEM) and thermal conductivity measurements. The effect of grain boundary segregation and second phase distribution on the thermal conductivity are discussed. The  $Er_2O_3$ -CaO- and the  $Yb_2O_3$ -CaO- AlN ceramics have a higher thermal conductivity than the CaO- and the  $Y_2O_3$ -CaO- AlN ceramics. This is explained on the basis of the free energy of formation ( $\Delta G^\circ$ ), the vaporization of the sintering additives and the microstructural development. Oxidation of freshly cleaned surfaces of those AlN ceramics was studied.

## 1. Introduction

Aluminium nitride (AlN) ceramics with the wurzite crystal structure have an excellent thermal conductivity, a high electrical resistivity and a low dielectric constant. The thermal expansion coefficient of AlN is an excellent match to silicon wafers in the temperature range of room temperature to 200 °C. The thermal conductivity of AlN is typically at least 5–6 times larger than that of alumina. AlN ceramics are therefore, ideal candidates as substrates for VLSI devices. However, the thermal conductivity of polycrystalline AlN containing additives has not been studied in detail. The presence of a second phase at grain boundaries, lattice-oxygen and defects in the sintered AlN ceramics are thought to be responsible for some observed effects. The use of additives is not only beneficial for achieving a high density, but also to enhance the thermal conductivity of the AlN ceramics. Many kinds of additives have been studied, although much of the work has been with CaO or  $Y_2O_3$  [1–5].

The purpose of this study is to investigate the microstructure of sintered AlN containing various oxides used as sintering aids using SEM and TEM techniques and to relate the observed microstructural features with the thermal conductivity of the sintered AlN. Furthermore, the oxidation phenomenon of a fresh clean AlN surface has been studied because of the importance of AlN surfaces for metallization.

## 2. Experimental procedure

Table I shows the chemical composition of the samples sintered with AlN powder (nitrogen 31.5 wt %, oxygen 2.83 wt %, carbon 0.26 wt % and particle size

of 3–5  $\mu\text{m}$ ) and oxide additives. The mixtures were blended for 24 h in a plastic jar using  $ZrO_2$  balls and an alcohol grinding medium. After the mixture was dried, it was granulated through an 80 mesh sieve and then pressed into a pellet. This pellet was immersed in AlN powder within a BN crucible. The specimens were sintered at 1900–2000 °C for 5–10 h in a nitrogen atmosphere.

The fracture surface of the sintered AlN ceramics was observed by SEM techniques. The TEM studies were conducted at a 200 kV accelerating voltage using a Philips model CM12 microscope. The sintered density was calculated using Archimedes' technique. The thermal conductivity was measured at room temperature by the laser-flush method.

## 3. Results

### 3.1. Microstructural development

Figs 1 and 2 show SEM fractographs of the AlN ceramics containing different sintering additives fired at 1950 °C for 5 h, 1900 °C for 10 h and 2000 °C for 5 h, respectively. The CaO AlN sample contains many

TABLE I The chemical composition of the AlN ceramics with additives

Sample	Content of additive (mol %)			
	CaO	$Y_2O_3$	$Yb_2O_3$	$Er_2O_3$
AC	1.5			
ACY	0.5	1.0		
ACYB	0.5		1.0	
ACER	0.5			1.0

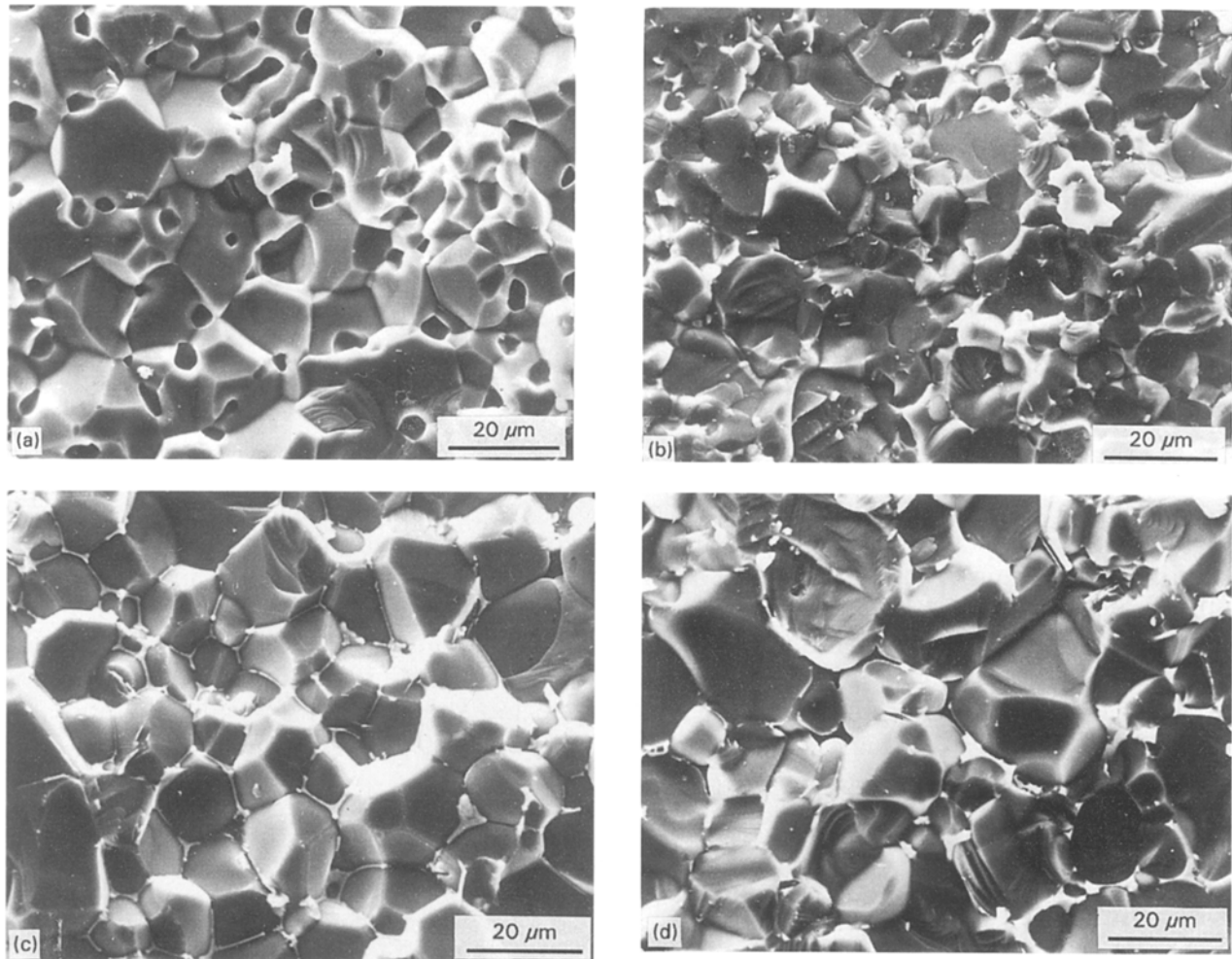


Figure 1 SEM fractographs of (a) CaO-, (b) Y<sub>2</sub>O<sub>3</sub>-CaO-, (c) Yb<sub>2</sub>O<sub>3</sub>-CaO- and (d) Er<sub>2</sub>O<sub>3</sub>-CaO-AlN ceramics fired at 1950 °C for 5 h.

pores and the porosity increases with increasing sintering temperature (Figs 1a and 2a). When the AlN ceramics were sintered at 1950 °C for 5 h, the grain size of the Yb<sub>2</sub>O<sub>3</sub>-CaO-AlN and the Er<sub>2</sub>O<sub>3</sub>-CaO-AlN ceramics is larger and more uniform than that of the Y<sub>2</sub>O<sub>3</sub>-CaO-AlN ceramic as is shown in Fig. 1. In the case of the Y<sub>2</sub>O<sub>3</sub>-CaO-AlN sample the grain size and the volume fraction of a second phase increased with increasing sintering temperature.

The Yb<sub>2</sub>O<sub>3</sub>-CaO-AlN sample was observed to have a similar grain size distribution (Figs 1b and 2b), but it retained a large amount of a second phase along the grain boundary when fired at 2000 °C for 5 h. As shown in Figs 1d and 2d, the grain size of the Er<sub>2</sub>O<sub>3</sub>-CaO-AlN sample fired at 1950 °C for 5 h was much larger than that of the sample heated at 1900 °C for 10 h that showed a continuous second phase at the grain boundary and a more narrow grain size distribution. It however contains less of the second phase at triple grain junctions.

### 3.2. Identification of the second phases

The sintered samples contain one or even two kinds of second phases in addition to the AlN main phase. Fig. 3 shows TEM selected area diffraction patterns of the AlN ceramics with additives fired at 1900 °C for 10 h or 1950 °C for 5 h. The second phase in the

CaO-AlN sample is identified as CaAl<sub>2</sub>O<sub>4</sub>·8.5H<sub>2</sub>O (Fig. 3a). From Fig. 3(b and c), the second phases of the Y<sub>2</sub>O<sub>3</sub>-CaO-AlN sample are identified as Y<sub>3</sub>Al<sub>5</sub>O<sub>12</sub> and Ca<sub>3</sub>Al<sub>2</sub>O<sub>6</sub>. In the case of the Yb<sub>2</sub>O<sub>3</sub>-CaO-AlN and the Er<sub>2</sub>O<sub>3</sub>-CaO-AlN ceramics, the second phase is Ca<sub>3</sub>Al<sub>2</sub>O<sub>6</sub> (Fig. 3(e and f)) and Θ-Al<sub>2</sub>O<sub>3</sub>, respectively. No aluminium ytterbium oxide, aluminium erbium oxide, ytterbium oxide and/or erbium oxide are found. Surface oxidation (Al<sub>2</sub>O<sub>3</sub> spot) is only observed in the Er<sub>2</sub>O<sub>3</sub>-CaO-AlN sample (Fig. 3f).

### 3.3. Density and thermal conductivity

The density and the thermal conductivity values of the sintered AlN ceramics are given in Table II. These values contrast with that of an hot-pressed pure AlN sample, in which the thermal conductivity is in the order of 50 W (m · k)<sup>-1</sup> [5]. The thermal conductivity of the Er<sub>2</sub>O<sub>3</sub>-CaO-AlN and the Yb<sub>2</sub>O<sub>3</sub>-CaO-AlN ceramics are higher than those of the CaO-AlN and the Y<sub>2</sub>O<sub>3</sub>-CaO-AlN ceramics. A firing temperature of 1900 °C is suitable for producing high thermal conductivity values.

The thermal conductivity exhibits an Avrami type [6] of behaviour. It is expected that the normalized thermal conductivity,  $\chi(t)$ , can be defined by;

$$\chi(t) = K(t) - K(0)/K(\infty) - K(0) \quad (1)$$

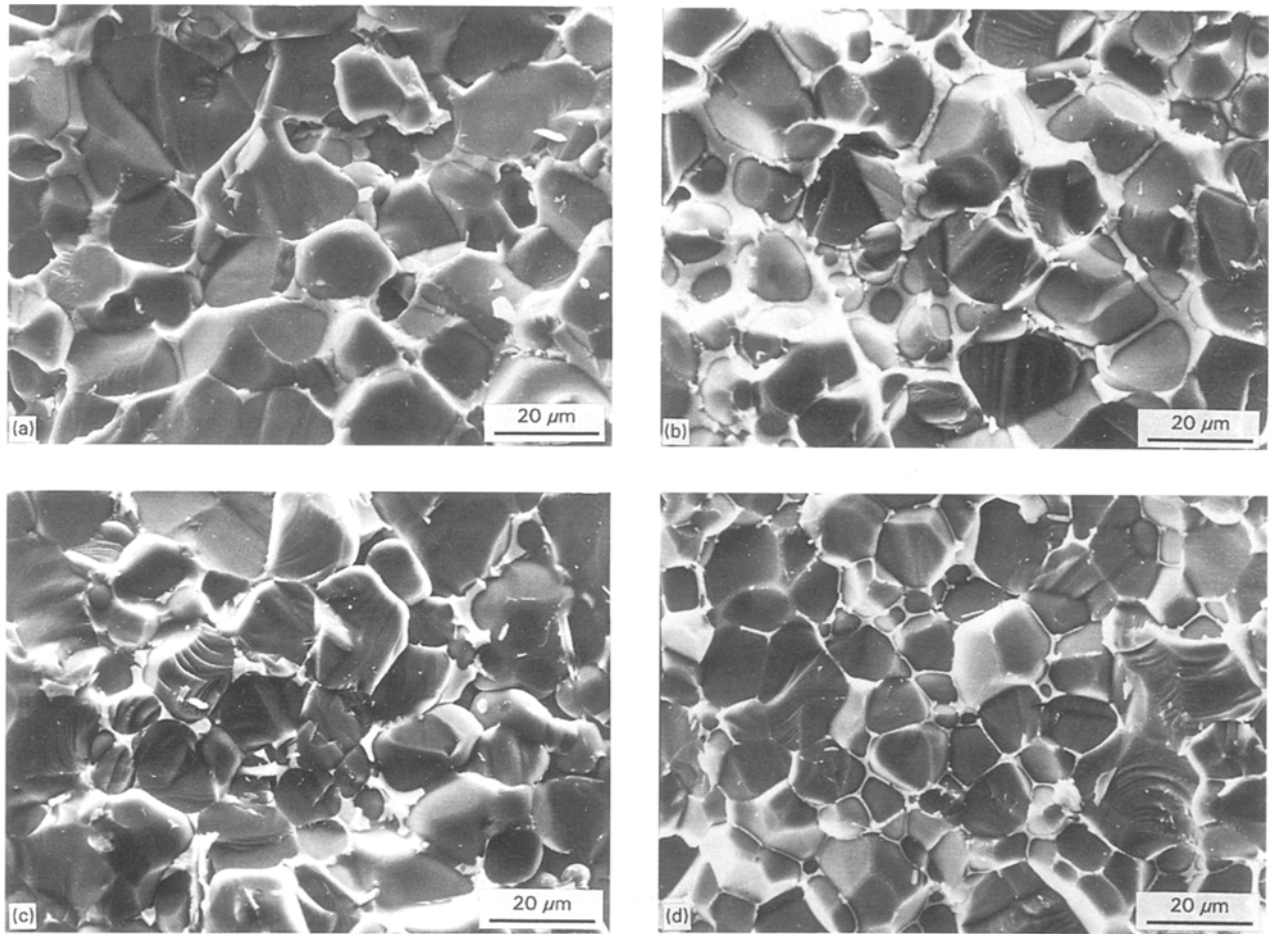


Figure 2 SEM fractographs of (a) CaO-, (b) Y<sub>2</sub>O<sub>3</sub>-CaO-, (c) Yb<sub>2</sub>O<sub>3</sub>-CaO- and (d) Er<sub>2</sub>O<sub>3</sub>-CaO-AlN ceramics, (a), (c), (d) were fired at 1900°C for 10 h, whilst (b) was fired at 2000°C for 5 h.

TABLE II The sintered density and thermal conductivity of the AlN ceramics with additives

Sample	Firing condition (°C-h)	Sintered density (g cm <sup>-3</sup> )	Thermal conductivity (W (m·k) <sup>-1</sup> )
AC	1950 - 5	3.19	-
	1900 - 10	3.22	74.3
ACY	1950 - 5	3.30	58.2
	2000 - 5	3.27	61.2
ACYB	1950 - 5	3.27	86.0
	1900 - 10	3.26	94.6
ACER	1950 - 5	3.20	91.7
	1900 - 10	3.30	112.4

and can then be expressed in terms of time,  $t$ , and the pertinent relaxation time,  $\tau$ , as follows:

$$\chi(t) = 1 - \exp[-(t/\tau)^m] \quad (2)$$

In Equation 1,  $K(0)$  is the initial thermal conductivity of the sample just after sintering.  $K(\infty)$  and  $K(t)$  are the thermal conductivity after long-term annealing and after one annealing for time,  $t$ , respectively. Equations 1 and 2 explain the observation that the longer the sintering temperature, the higher the observed

thermal conductivity. The results in Table II are consistent with Equations 1 and 2.

## 4. Discussion

### 4.1. Microstructure and thermal conductivity

The thermal conductivity of a multiphase material depends not only on the thermal conductivity of the individual phases, but also on the distribution of these phases. When the AlN matrix and the grain boundary phases are continuous, the thermal conductivity of the multiphase material can be described as follows [7];

$$K = K_m(1 - V_v) + K_{gb} V_v \quad (3)$$

where  $K_m$  and  $K_{gb}$  are the thermal conductivity of the AlN matrix and the grain boundary phase, respectively, and  $V_v$  is the volume fraction of the grain boundary phase. Therefore, the reason why the Er<sub>2</sub>O<sub>3</sub>-CaO-AlN and Yb<sub>2</sub>O<sub>3</sub>-CaO-AlN ceramics have a higher thermal conductivity than those of Y<sub>2</sub>O<sub>3</sub>-CaO-AlN and CaO-AlN ceramics is explained by the point that the former have less of the grain boundary phase in comparison with the latter as is shown in Fig. 2. Furthermore, the CaO-AlN sample could not be used as a substrate material due to the presence of pores in the bulk. These pores inhibit the improvement of the thermal conductivity.

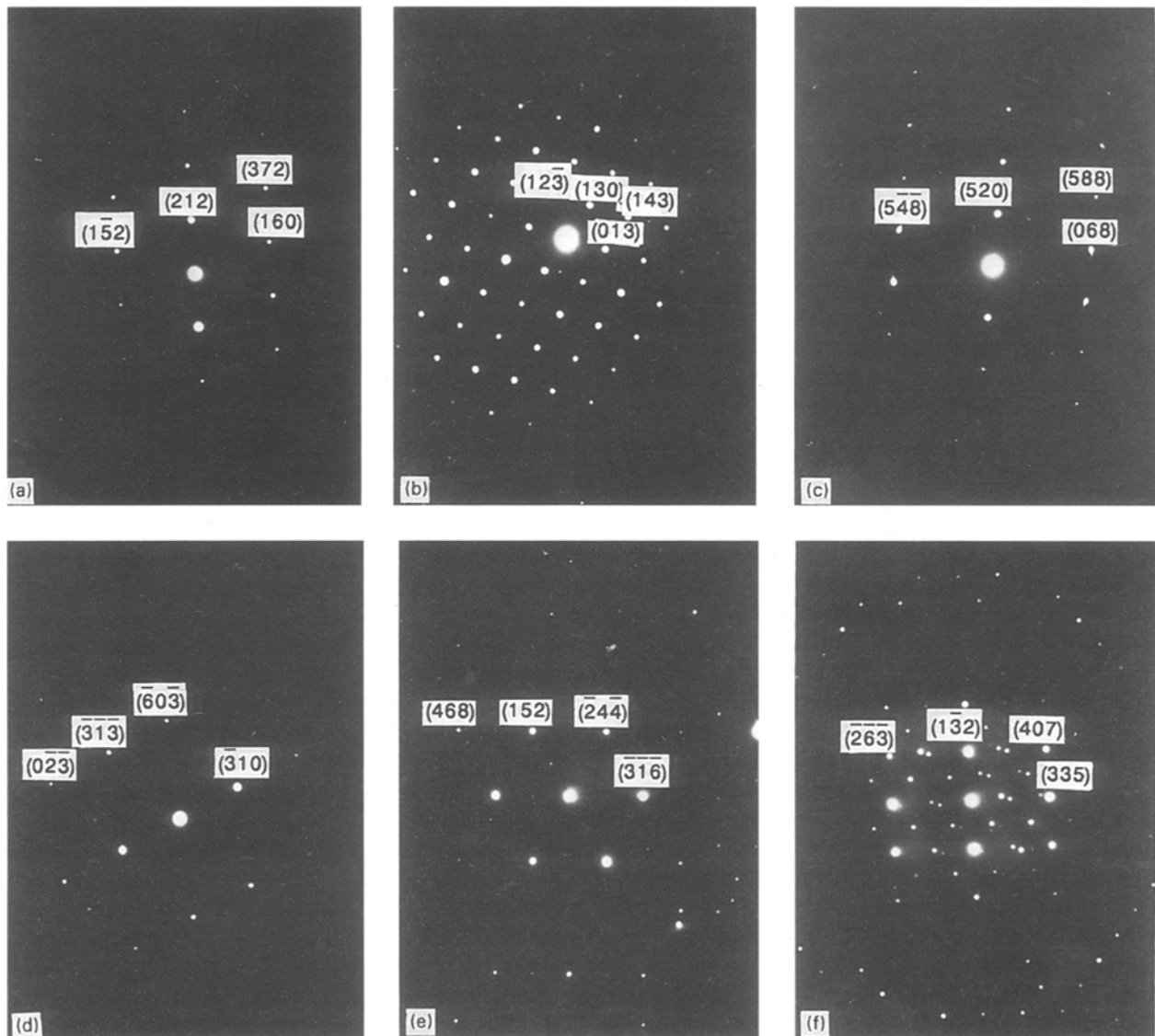


Figure 3 TEM selected area diffraction patterns of the samples of (a) Fig. 2a, (b) and (c) Fig. 1b, (d) Fig. 2c, (e) and (f) Fig. 2d, respectively.

#### 4.2. Second phase and thermal conductivity

Samples with a high thermal conductivity value could be obtained in the absence of a second phase at the grain boundary and also of oxygen as an impurity in the bulk [8]. The mechanisms for impurity oxygen removal include; (a) impurity such as  $\text{Al}_2\text{O}_3$  in the  $\text{AlN}$  matrix could diffuse into the grain boundary and react with the sintering additives such as  $\text{CaO}$ ,  $\text{Y}_2\text{O}_3$ ,  $\text{Yb}_2\text{O}_3$  and  $\text{Er}_2\text{O}_3$  to form a liquid phase that assists in densification. (b) The oxide liquid phase transports to the surface of the sample and vaporizes at high temperatures. Second phases of ytterbium oxide, aluminium ytterbium oxide, erbium oxide and aluminium erbium oxide are not found in the  $\text{Yb}_2\text{O}_3$ - $\text{CaO}$ - $\text{AlN}$  and the  $\text{Er}_2\text{O}_3$ - $\text{CaO}$ - $\text{AlN}$  ceramics as shown in Fig. 3 even though aluminium yttrium oxide was formed and remained at the grain boundary under the same firing conditions. The values of evaporation of  $\text{Yb}_2\text{O}_3$  and  $\text{Er}_2\text{O}_3$  are  $2.3 \times 10^{-5} \text{ g cm}^{-2} \cdot \text{sec}^{-1}$  and  $1.2 \times 10^{-5} \text{ g cm}^{-2} \cdot \text{sec}^{-1}$ , respectively, which are three orders of magnitude higher than that of  $\text{Y}_2\text{O}_3$  ( $8 \times 10^{-8} \text{ g cm}^{-2} \cdot \text{sec}^{-1}$ ).

It has been suggested that additions of  $\text{CaO}$  may enhance the vapour phase transport of  $\text{Al-O}$  species

[9]. From the experiment on the weight loss between  $\text{CaO-Al}_2\text{O}_3$  samples and pure  $\text{Al}_2\text{O}_3$  specimens, it was demonstrated that the weight loss of  $\text{CaO-Al}_2\text{O}_3$  specimens not only exceeded ten times that of the pure  $\text{Al}_2\text{O}_3$  specimen, but also far exceeded the total amount of  $\text{CaO}$  addition: This means that a substantial volatilization of  $\text{Al}_2\text{O}_3$  does not occur in the absence of  $\text{CaO}$  addition. In the  $\text{Yb}_2\text{O}_3$ - $\text{CaO}$ - $\text{AlN}$ , it was shown by TEM analysis that the addition of  $\text{Yb}_2\text{O}_3$  may enhance the volatilization of  $\text{CaO}$ . Therefore the  $\Theta$ - $\text{Al}_2\text{O}_3$  remaining at the grain boundaries presumably due to the absence of  $\text{CaO}$  (Fig. 3f). This remaining  $\text{Al}_2\text{O}_3$  phase produces the lower thermal conductivity in comparison with the  $\text{Er}_2\text{O}_3$ - $\text{CaO}$ - $\text{AlN}$ . More detailed experiments exploring this phenomenon are under investigation.

From a thermodynamic viewpoint, the greater the affinity of the additives for  $\text{Al}_2\text{O}_3$ , the greater the degree of purification of the  $\text{AlN}$  lattice. The affinity can be quantified in terms of the standard free energy of formation,  $\Delta G^\circ$ , of the respective aluminate. Therefore, the higher the  $|\Delta G^\circ|$ , with  $\Delta G^\circ < 0$ , the higher the affinity. Correspondingly, the thermal conductivity

of the sintered AlN ceramics will be higher. The higher thermal conductivity values for samples with additives of Er<sub>2</sub>O<sub>3</sub> and Yb<sub>2</sub>O<sub>3</sub> (Table II) would suggest that Er<sub>2</sub>O<sub>3</sub> and Yb<sub>2</sub>O<sub>3</sub> are probably more effective at removing oxygen than is Y<sub>2</sub>O<sub>3</sub>. However, it is difficult to make a definite conclusion without relevant thermodynamic data.

#### 4.3. Oxidation of a freshly cleaned surface of AlN

It is difficult to metallize a clean surface of an AlN ceramic especially with thick or thin films of Cu. The peel strength of Cu metallization was significantly improved when a thin Al<sub>2</sub>O<sub>3</sub> layer was present on the surface of the AlN. A freshly clean surface of an Er<sub>2</sub>O<sub>3</sub>-CaO-AlN ceramic is found to be susceptible to oxidation even at room temperature, but no ambient temperature oxidation is found on any other sample. These results suggest that the activity of AlN in the Er<sub>2</sub>O<sub>3</sub>-CaO-AlN system is higher than that in the other AlN samples. All the AlN samples except for the Er<sub>2</sub>O<sub>3</sub>-CaO-AlN sample needed to be heated in order to obtain a thin Al<sub>2</sub>O<sub>3</sub> layer.

#### 5. Conclusion

AlN ceramics with the addition of Er<sub>2</sub>O<sub>3</sub>-CaO and Yb<sub>2</sub>O<sub>3</sub>-CaO have a higher thermal conductivity and a lower second phase content than those with Y<sub>2</sub>O<sub>3</sub>-CaO and solely CaO additions. The CaO-AlN material showed many pores, and thus it cannot be used as a substrate material. The second phase in the CaO-AlN sample is identified as CaAl<sub>2</sub>O<sub>4</sub>·8.5H<sub>2</sub>O,

in the Yb<sub>2</sub>O<sub>3</sub>-CaO-AlN sample as  $\Theta$ -Al<sub>2</sub>O<sub>3</sub> and in the Er<sub>2</sub>O<sub>3</sub>-CaO-AlN sample as Ca<sub>3</sub>Al<sub>2</sub>O<sub>6</sub>. The second phases in the Y<sub>2</sub>O<sub>3</sub>-CaO-AlN sample are Y<sub>3</sub>Al<sub>5</sub>O<sub>12</sub> and Ca<sub>3</sub>Al<sub>2</sub>O<sub>6</sub>. No aluminium ytterbium oxide, aluminium erbium oxide, ytterbium oxide or erbium oxide is observed. Ambient temperature oxidation is found only on the freshly cleaned surface of the Er<sub>2</sub>O<sub>3</sub>-CaO-AlN sample. In order to obtain a thin layer of Al<sub>2</sub>O<sub>3</sub> that improves the peel strength of Cu metallization to AlN ceramics, all the AlN samples except for the Er<sub>2</sub>O<sub>3</sub>-CaO-AlN sample needed to be heated.

#### References

1. T. B. TROCZYNSKI and P. S. NICHOLSON, *J. Amer. Ceram. Soc.* **72** (1989) 1488.
2. T. YAGI, K. SHINOZAKI, N. MIZUTANI, M. KATO and A. TSUGE, *J. Mater. Sci.* **24** (1989) 1332.
3. K. KOMEYA, A. TSUGE, H. INOUE and H. OHTA, *J. Mater. Sci. Lett.* **1** (1982) 325.
4. N. S. VAN DAMME, S. M. RICHARD and S. R. WINZER, *J. Amer. Ceram. Soc.* **72** (1989) 1409.
5. S. PROCHZKA and C. F. BOBIK, in "Sintering of Aluminum nitride," in *Materials Science Research*, Vol. 13 (Plenum Press, New York and London, 1979) p. 321.
6. E. FINE, in "Introduction of Phase Transformations in Condensed Systems," (McMillan Press, New York, 1964).
7. A. VIRKAR, T. B. JACKSON and R. A. CUTLER, *J. Amer. Ceram. Soc.* **72** (1989) 2031.
8. G. A. SLACK, *J. Phys. Chem. Solids* **34** (1973) 321.
9. R. F. FUENTES, Ph.D. thesis, Massachusetts Institute of Technology, Cambridge (1986).

*Received 10 August*

*and accepted 21 December 1995*